Modeling Turbulence Control Effect of the SINHA Flexible Composite Surface Deturbulator

Xiao Wang[1], Keith Walters[2], Lorenzo Coley[3], Michael Barton[4]
Mississippi State University, Miss. State, MS, 39762

and

Sumon Sinha[5]
SinhaTech, Oxford, MS, 38655

The effect of treating an aerodynamic surface with a Flexible Composite Surface Deturbulator (FCSD) has been modeled using Loci/CHEM, a RANS CFD code. The FCSD is postulated to control turbulent mixing by utilizing its ridged substrate to break up long wavelength flow instabilities imposed on its flexible surface. To mimic this cost-effectively, a turbulence length scale limiter has been selectively applied to the k-ω turbulence model, thereby constraining the length scale of turbulence production. CFD predictions of a Deturbulator treated deflector oriented 30 degrees with respect to the freestream validate the wave breakdown effect when compared to wind tunnel measurements. Simulations of a S809 wind turbine airfoil have yielded modified 20% lower low-skin friction marginally separated boundary layers over 95% of the chord on the upper surface, and a 2% increase in L/D.

Nomenclature

D	=	Drag
fl	=	User specified factor determining zone of influence
k	=	Turbulent kinetic energy
L	=	Lift
l	=	Turbulence (mixing) length scale
l_{max}	=	Limiting value of turbulence length scale
l_t	=	Non-dimensional turbulent length scale
p	=	Pressure
r	=	eddy radius
U	=	Mean Velocity Component
u	=	Fluctuating Velocity Component
x_i	=	Spatial coordinate in direction i
y	=	Distance from the wall or cross-stream coordinate
ω	=	Vorticity

[1] Assistant Research Professor, Center for Advanced Vehicular System, Mississippi State University, Mail Stop 9618, Mississippi State, MS 39762. Tel: 662-325-1009

[2] Associate Professor, Department of Mechanical Engineering and Center for Advanced Vehicular System, Mississippi State University, Mail Stop 9618, Mississippi State, MS 39762. Tel: 662-325-8231

[3] Instructor, Department of Aerospace Engineering, Mississippi State University, P.O. Drawer A, Mississippi State, MS 39762. Tel: 662-325-1012

[4] Undergraduate Student of Aerospace Engineering, Mississippi State University, P.O. Box 856, Mississippi State, MS 39762. Tel: 901-485-1464

[5] President, SINHATECH and Adjunct Professor of Aerospace Engineering, Mississippi State University, 3607 Lyles Drive, Oxford, Mississippi 38655. Tel: 662-801-6248

I. Introduction

A flexible composite surface Deturbulator (FCSD), shown in Fig. 1, has been invented[1] and developed at SINHATECH. This Deturbulator is a thin passive device consisting of a flexible membrane stretched across an array of ridges on a substrate that can be attached to an aerodynamic surface. The membrane undergoes extremely small flow-induced flexural oscillations. These are postulated to neutralize turbulent fluctuations in the near-wall boundary layer and reduce turbulent mixing in separated wakes. In-flight and wind tunnel tests conducted by SINHATECH on a wing section with an applied FCSD showed significant reductions in drag and increases in lift[2]. Statistically significant fuel savings were observed for trucks with applied FCSDs as well[3]. Even though the aforementioned studies and other macro observations suggest that the Deturbulator modifies the turbulence spectrum by directly breaking down the larger turbulent eddies into smaller ones, the details of the process are extremely difficult to observe and quantify. Methods which can capture the required large scales cannot resolve the sub-micron smaller scales. Optimizing Deturbulator performance requires painstaking matching of surface geometry with flow conditions on the flexible surface. At present this necessitates repeated tests on the prototype. Simulations using high-fidelity CFD software is therefore needed to cost-effectively predict the impact of the Deturbulator in flows of interest. This work presents an approach for achieving this in order to enable wide spread adoption of Deturbulator flow control.

a). Deturbulator Insert Schematic   b). Slide in Deturbulator Insert with Flexible Composite Surface

Figure 1. Structure of the FCSD Deturbulator

II. Large-Eddy Break-Up with Flexible Surface Deturbulators

The ability to control turbulence, or attenuate turbulence levels (i.e., "de-turbulate") without introducing added device drag can open new vistas in manipulating fluid flow. One area that immediately opens up is the ability to virtually shape an object by adding areas of stagnated separated zones. Such shaping can be used to reduce drag or increase lift.

Normally an area of separated boundary layer flow has extremely high rate of dissipation of flow mechanical energy. This is initiated by the formation of large vortices and their subsequent breakdown into smaller and smaller vortices through the turbulent energy cascade[4]. The smallest vortices at the tail end of the cascade have the highest rate of dissipation of flow kinetic energy into heat. By reducing the energy available for the largest vortices the entire cascade can be modified so as to lower the highest dissipation rate. This requires reducing the magnitude of the Turbulent Kinetic Energy Production term, given by:

$$-\langle u_i u_j \rangle\, \partial U_i / \partial x_j$$

Such a reduction will require reducing the magnitude of $\langle \boldsymbol{u_i u_j} \rangle$ in the anisotropic shear layer driving the large vortices.

If one assumes such a shear layer to be aligned in direction 1 with gradients across direction 2, wave breaking process in the shear layer will be the primary source for fluctuations $\langle \boldsymbol{u_1} \rangle$ in direction 1. Fluctuations in directions 2 and 3 can only be introduced through the pressure-strain rate transport terms:

$$\langle p\, \frac{\partial u_1}{\partial x_1} \rangle = -\left[\langle p\, \frac{\partial u_2}{\partial x_2} \rangle + \langle p\, \frac{\partial u_3}{\partial x_3} \rangle \right]$$

American Institute of Aeronautics and Astronautics

If one can reduce the wavelengths of the instabilities prior to break up the resulting eddy or vortex will have a smaller diameter 2$\mathbf{r}$. For a given mean flow gradient $\partial U_1/\partial x_2$, $\langle u_1 \rangle$ will be of the order $(2r \cdot \partial U_1/\partial x_2)$. Hence, the magnitude of $\langle u_i u_j \rangle$ and the rate of production of turbulent kinetic energy will come down as a result of premature wave breaking.

There are many ways one can break up large turbulent eddies in shear flows, such as screens[4]. Unlike the Flexible Composite Surface Deturbulator, most boundary layer Large Eddy Breakup (LEBU) devices protrude away from the wall[5]. Both screens and traditional LEBU devices increase flow blockage and add "device drag". The postulated mechanism of direct breakdown of instability waves by the Deturbulator has been described by Sinha and Hyvarinen[6]. Furthermore, the instability wave breakdown mechanism also influences the shear layer after the boundary layer separates. This is in line with reducing turbulent dissipation in separated flows as outlined in the previous paragraph.

The effect of reduction of turbulence in the separated wake behind a Deturbulator-enhanced wind-deflector[7] has been documented in videos[8]. Skin friction drag on streamlined objects can be lowered by intentionally inducing marginal boundary layer separation while limiting the onset of pressure drag by controlling turbulence. For example, using a Deturbulator tape on the top surface of a sailplane wing has been found to enhance the best lift-drag ratio (L/D) by 18% in independently validated flight tests[9]. Oil flow visualization has shown evidence of stagnated separated flow on the wing[10]. Deturbulators have also been found to improve fuel economy of tractor trailer trucks by more effectively hiding the load on an open trailer in more stagnant air, or by more effectively shielding the front face of a van-trailer within a stagnated separated zone[3,11].

Even though the basic mechanism for drag reduction appears to follow the logic stated in the aforementioned sections, no detailed computational study of the phenomena has been attempted until now. The ability to model the effect of the Deturbulator in a cost effective manner is critical for optimizing its integration. At present the procedure for optimization requires extensive experimentation, which is not cost effective in many cases.

The focus of this paper is to address this shortcoming. It is a pioneering investigation based on modification of the mixing length parameter in a RANS code and represents work in progress. This approach has been validated by comparing computational results with data obtained from wind tunnel experiments.

III.   Wind Tunnel Experiment

A. Hardware Specifications
The wind tunnel tests were performed in the subsonic wind tunnel in Patterson labs at Mississippi State University. It is a closed loop wind tunnel with an open test section. The test section has dimensions of three feet in width, four feet in height, and five feet in length. The current limit of the tunnel is 160 feet per second or approximately 110 miles per hour.

Figure 2. Deturbulator Test Model in Wind Tunnel

The Deturbulator strip (including the backing and slide-in Deturbulator insert) was mounted onto a flat plate, which is shown in Fig. 2. The Deturbulator strip had overall dimensions of 24.125 inches span by 3.5 inches chord. The plate that it was mounted on had a span of 21.188 inches and a streamwise length of 14.625 inches. Smooth red tape was used to hinge the leading edge of the Deturbulator strip to the plate. The tape also helped make a smooth transition from the plate to the bottom of the Deturbulator strip. A bolt was used to adjust and hold the Deturbulator strip at the desired angle, which for all the tests reported here was 30 degrees. The last piece that was added was a small diameter rod to the leading edge of the plate to eliminate flow separation off the sharp edges of its blunt

American Institute of Aeronautics and Astronautics

surface. In addition to testing the flexible surface Deturbulator, a hard smooth-surface plastic insert with the same profile and size was also tested to see how the wake velocity profiles changed.

Velocity profiles were measured using a single wire hotwire probe. The probe was a TSI model 1218-20. The probe was attached to a TSI model 1750 constant temperature anemometer, which then output voltages. A National Instruments USB-6251 data acquisition device, with a 16 bit resolution and a maximum sampling rate of 1.25 megasamples per second was used to record the voltages. For all the tests that were performed, the DAQ device was set at a sampling rate of 10,000 Hz and 10,000 samples, recording data over a total period of 1-second at each position of the probe. The samples were then averaged to get an average velocity at that point. Finally, the hotwire probe was attached to a three axis traverse to allow for movement of the probe.

B. Data Collection

Two separate LABVIEW programs were used to collect and analyze the data from the hotwire. The first program controlled the traverse as well as recorded the data from the hotwire. This program allowed for two different types of input. The first one was to manually type in coordinates, and the second was for the program to read in a coordinate file. The latter was used in the wind tunnel tests. Before creating the coordinate file, a starting point had to be determined.

The starting point was chosen to be one inch above the flat plate in the z-direction, one inch behind the tip of the Deturbulator in the streamwise x-direction, and halfway between the bolt that held the Deturbulator in place and the tip of the plate in the y-direction. The y coordinate was chosen to try and minimize flow disturbance due to the bolt and the tip of the plate. This coordinate remained the same for all the tests. The vertical or z-coordinate was adjusted in two separate intervals. From one inch above the plate to 2.95 inches above the plate, the interval was 0.05 inches. From 2.95 inches to 10.45 inches, the interval was 0.25 inches. The reason for separate intervals was that the region slightly above and below the trailing edge of the Deturbulator was the desired capture region. However, continuing at this interval for the rest of the vertical coordinates would require more data points, which would require very long test runs. The downstream or x-coordinate was also changed. The coordinates chosen for this coordinate was 1, 2, 5, and 10 inches downstream of the trailing edge of the Deturbulator strip. These captured the streamwise development of wake velocity profiles.

The outputs from this program consisted of average velocity and the samples that were taken. Another LABVIEW program performed a statistical analysis of the data. Several statistical values were examined. One in particular was a turbulence factor as shown in Fig. 3, which was found by dividing the root mean squared value by the mean value. The graph shows that the freestream turbulence factor is around one. However, the factor increases when the hotwire is around the trailing edge of the Deturbulator strip. At ten inches, the factor does not increase as much. This is due to the fact that the flow has started to re-stabilize.
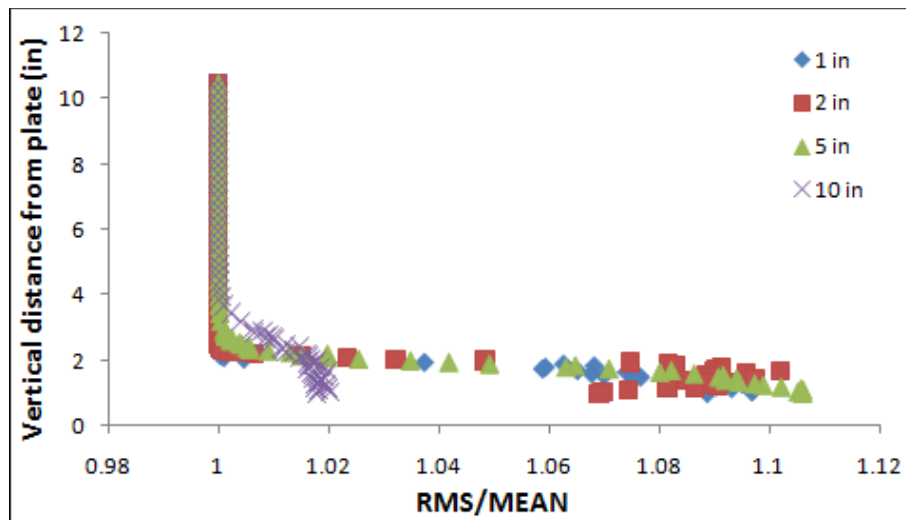
Figure 3. Turbulence Factor

American Institute of Aeronautics and Astronautics

IV. CFD Modeling of the Flexible Surface Deturbulator

This work aimed at modeling the influence of the Deturbulator on flows. Flow-induced oscillation of the Deturbulator membrane is not simulated directly since it is not practical and far beyond the expense appropriate for this very preliminary stage of research. Instead, an approach that limits the turbulence length scale to a specified maximum value has been adopted in the turbulence model to mimic capping the size of turbulent eddies. The Loci/CHEM code, an in-house, unstructured, finite-volume RANS solver was used. This Mississippi State CFD code that has been used previously for a wide variety of aerodynamic simulations[12,13].

In order to correctly model the flow, the turbulence model has to be selectively changed to manipulate the turbulence length scale near FCSD-treated surfaces. The simplest way to model this phenomenon is to prescribe a limit for the maximum mixing length for regions that are affected by the Deturbulator. Hence, an additional parameter has been introduced; namely the distance from the wall where the maximum mixing length criterion is to be applied. Depending on the outcome of this approach, a region near the Deturbulator with streamwise extent corresponding to the chord size of the Deturbulator strip can be used to account for changes in placement and the size of the Deturbulator strip. Prior experiments have revealed that placement and size are critical to the overall performance (e.g., drag reduction) resulting from use of the Deturbulator. Placement and size are also affected by the variation of laminar separation bubbles with lift and Reynolds number and incorrect placement can degrade performance.

A. Turbulent Model and Length Scale Limiting

In the turbulence model, a lower limit is applied to the scale-determining variable, ω, which is equivalent to an upper limit on turbulence length scale. To model the impact of a Deturbulator-treated aerodynamic surface, the surface should be identified and distinguished from regular viscous surfaces.

Length scale varies throughout boundary layer flow field. Definition of the turbulence length scale $l = \sqrt{k}/(0.09 \times \omega)$, and its non-dimensional form, $lt = \sqrt{k}/(0.09 \times \omega \times y)$ used in Menter's BSL model are adopted in the current work, where y is the distance to the nearest wall surface. l_t is equal to 2.5 in the log layer and goes to zero towards the boundary layer edge. Thus a user-defined factor fl is introduced as

$$lt = \sqrt{k}/(0.09 \times \omega \times y) > fl \tag{1}$$

to constrain the Deturbulator's influence to a region near the wall but beyond a specified distance from the wall. Within this influence zone, it is assumed that turbulence eddies can break into smaller ones. The size reduction of turbulence eddies is modeled by introducing an upper bound of turbulence length scale, $l_{max,}$ such that

$$\omega d = \max(\omega, \frac{\sqrt{k}}{0.09 \times lmax}) \qquad \text{if } lt > fl \tag{2}$$

Here ω represents the variable in the original turbulence model, and ωd is the one that considers the effect of the Deturbulator oscillations.

B. Simulation of the Deturbulator Strip Model in the Wind Tunnel

A mixed-element type unstructured grid suitable for viscous simulations was generated for the test model using SolidMesh[14] and AFLR[15,16] grid generation software. The upstream, and downstream boundary surfaces are 29.625, and 80 inches from the leading edge of the test model, respectively. The top and bottom boundaries were 25.75, and 11 inches from the mounting plate, respectively. Two symmetric boundary surfaces are created along the span direction separated by a distance of 0.1 inches. The normal spacing of the first grid point off the mounting plate and test model surfaces is within a dimensionless distance of y+ < 1.0 to ensure viscous sublayer resolution. Prism cells are generated in the viscous layer to a distance off the surface based on an estimated boundary layer thickness. Figure 4 shows one of the symmetric boundaries in the grid.

At this stage, the major objective was to seek any qualitative characteristics in the resolved flow field obtained using the length-scale limiter in the Menter's BSL two-equation k-ω turbulence model[17]. Simulations using the standard BSL model and the scale limiter algorithm were conducted. The test case is the Deturbulator strip at 30° deflection in 55 mph sea-level air. Simulation using the standard BSL turbulence model was performed first to obtain a base-line flow corresponding a rigid-surface insert test model. Detailed distributions of the length scales l_t and l in the boundary layer are plotted in Figs. 5 and 6, respectively. The dimensional length scale l was found to be 0.006 m at the outer edge of the boundary layer. Based on this value, the second simulation enforced a reduction of

maximum length scale l_{max} = 0.002 m to model the Deturbulator's impact. As discussed herein above, the parameter fl defines an influence zone within the boundary layer over the Deturbulator. In the second simulation, a value of fl=0.5 is tried to allow the Deturbulator's impact to go beyond the log layer. The resulting boundary layer length scales are presented in Fig. 7. Since the wind-tunnel tests conducted up to this point could not perform measurements within the boundary layer due to limitations imposed by the available probe mount, parameters l_{max} and fl have to be specified arbitrarily. In spite of this shortcoming the effect of l_{max} and fl specifications on numerical solutions could be investigated.
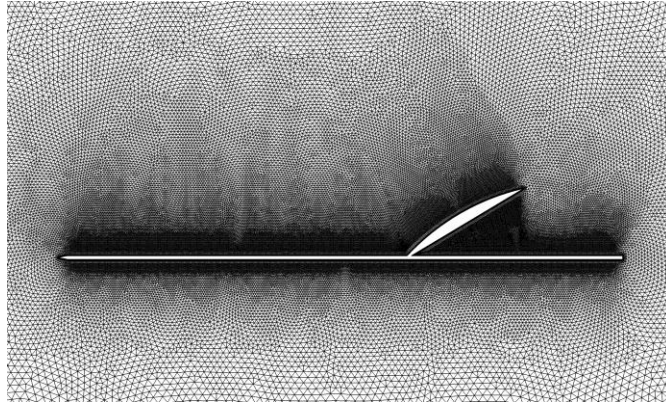
Figure 4. Computational Mesh of Deturbulator Model Tested in Wind Tunnel
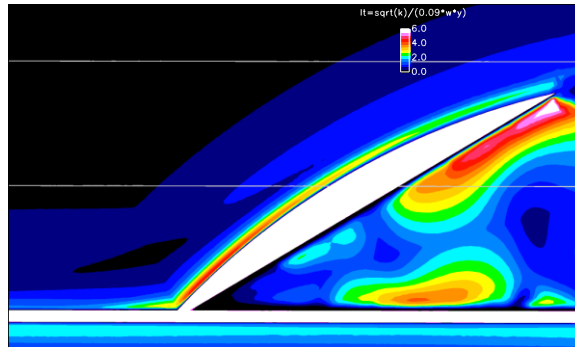
Figure 5. Contours of Length Scale l_t in the Boundary Layer Using Standard BSL model
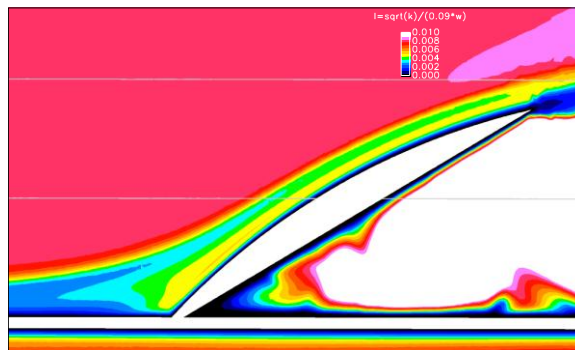
Figure 6. Contours of Length Scale l in the Boundary Layer using Standard BSL model

In the wind tunnel test, the test model had either rigid (clean) surface or with the Deturbulator attached. The vertical distributions of wake velocity magnitudes, as shown in Fig. 8, were measured at four locations, which are 1,

2, 5, and 10 inches aft of the trailing edge of the Deturbulator strip. The test model geometry can be found in Fig. 9, which also shows the flow field calculated using the standard BSL model. Both wind tunnel test and CFD simulation show that a maximum velocity magnitude occurs in the wake right behind the model surface. A close up view in this region also indicates that the use of a Deturbulator reduces the velocity magnitude; even though the amount of reduction was moderate in the current wind-tunnel test, such as 1% at 1-inch, 2.5% at 2-inch, 4% at 5-inch and 3% at 10-inch locations.
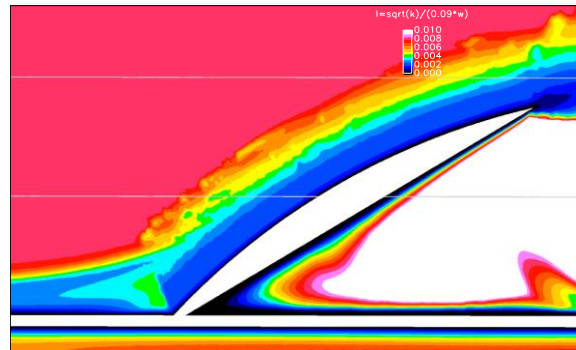
Figure 7. Contours of Length Scale l in the Boundary Layer Using Limiter $lmax = 0.002$ for Region where $lt > 0.5$

a) Full view   b) Close up view
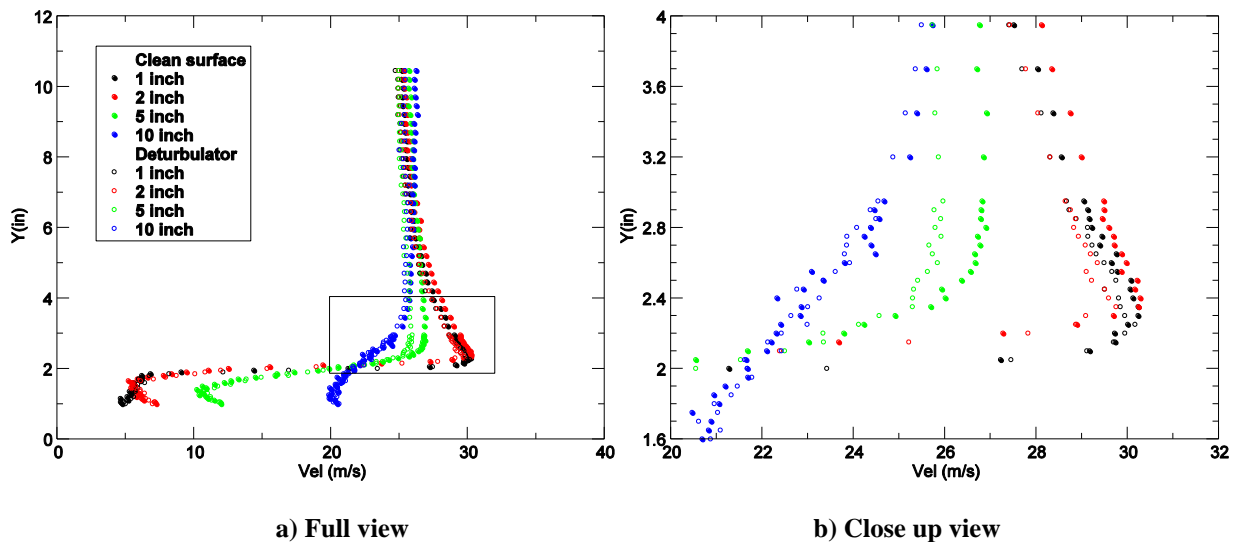
Figure 8. Total Velocity Profiles Measured in Wind-Tunnel Test

The predicted flow fields using the standard BSL turbulence model (BSL) and the length-scale limiter (LSL) are presented by the contours of velocity magnitude in Figs 9 and 10, respectively. Corresponding velocity profiles are plotted in Fig. 11. Comparing the two solutions, it is encouraging to see that the LSL simulation, as well, reduced the magnitude of total velocity in the wake region. This result matches the tendency observed in the wind-tunnel test and in the video[8]. Consequently, LSL altered the pattern of vortex shedding.

Before the current algorithm is able to aid the design and application of the Deturbulator device, issues about the specifications and behaviors of parameter fl and $lmax$, and their relationships to flow conditions and problem scales remain to be resolved.

American Institute of Aeronautics and Astronautics
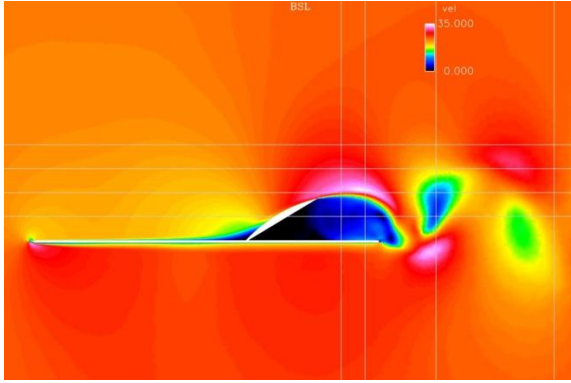
Figure 9. Velocity Magnitude by BSL
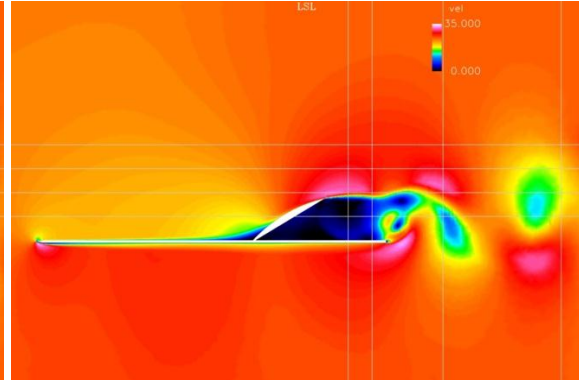
Figure 10. Velocity Magnitude by BSL_LSL

a) Full view

b) Close up view
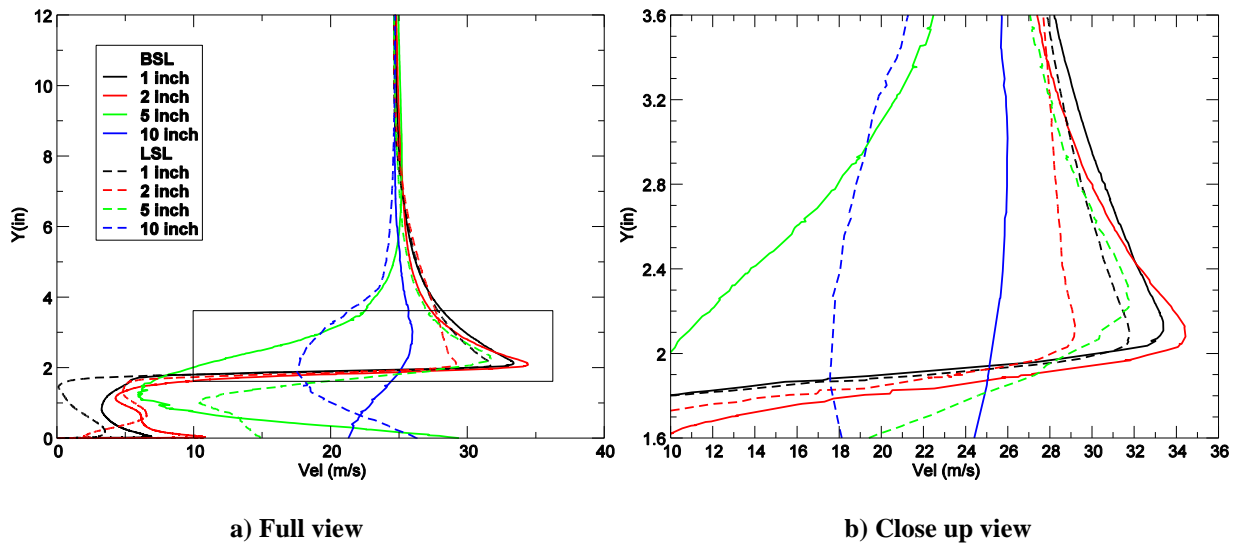
Figure 11.   Total Velocity Profiles Predicated by BSL and BSL_LSL Models

C. Simulation of Deturbulator-Treated Airfoil S809

In order to provide baseline flows to guide applications of the Deturbulator, it is essential to resolve viscous boundary layer flows, especially as flow separation and laminar-turbulent transition are involved. The key numerical technique for this task is the transition-sensitive turbulence model[19] (TSM). This model is a three-equation eddy viscosity type, with transport equations solved for turbulent kinetic energy (k_T), specific dissipation rate (ω), and laminar kinetic energy (k_L). This is one of the most practical turbulence models, which do not require non-local information in the boundary layers to resolve the turbulent transition. In the model, the transition process itself is represented as a transfer of energy from the laminar kinetic energy to the turbulent kinetic energy. Details of the model derivation and equations, as well as further validation test cases, are available in Ref. 18. The LSL algorithm is implemented in the TSM turbulence model to model the Deturbulator impact on flows undergoing laminar turbulent transition.

The S809 airfoil is a laminar-flow airfoil that was designed specifically for horizontal axis wind-turbine applications[19]. This airfoil has been tested in the low-turbulence wind tunnel at Delft University of Technology, Netherlands. The turbulence level in the wind tunnel test section varies from 0.02% at 10 m/s to 0.04% percent at 60 m/s. Wind tunnel test show that flow undergoes laminar separation followed by a turbulent reattachment. At Reynolds number of 2×10^6 and an angle of attack of 5.13º, the lift coefficient corresponds approximately to the upper limit of the laminar bucket. As the angle of attack is increased further, turbulent trailing edge separation occurs on the upper surface.

All CFD simulations in the current work are conducted at Reynolds number of 2×10^6 and an angle of attack of 5.13º. An estimated turbulence intensity of 3.55% based on the incoming flow speed is employed. Unstructured viscous meshes are generated with various resolutions for grid refinement study. According to wind tunnel test, turbulent transition on the upper surface occurs between 40%-50% chord. The final grid (Fig. 12) has grid spacing packed between 40%-60% chord on both upper and lower surfaces, which assured the capture of turbulent transition in this region. The CFD simulation using the TSM turbulence model achieved good agreement with the wind tunnel test data, which was indicated by the pressure coefficients shown in Fig. 13.
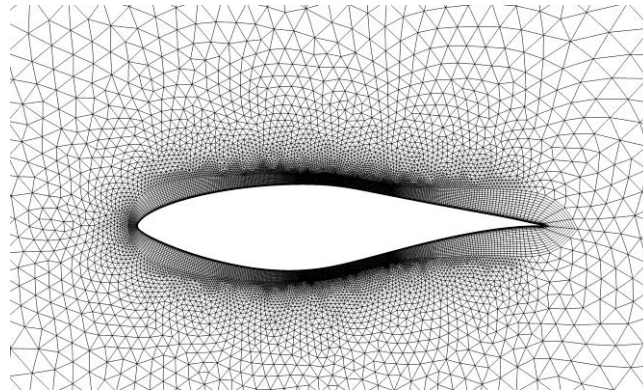
Figure 12. Geometry and Mesh of S809
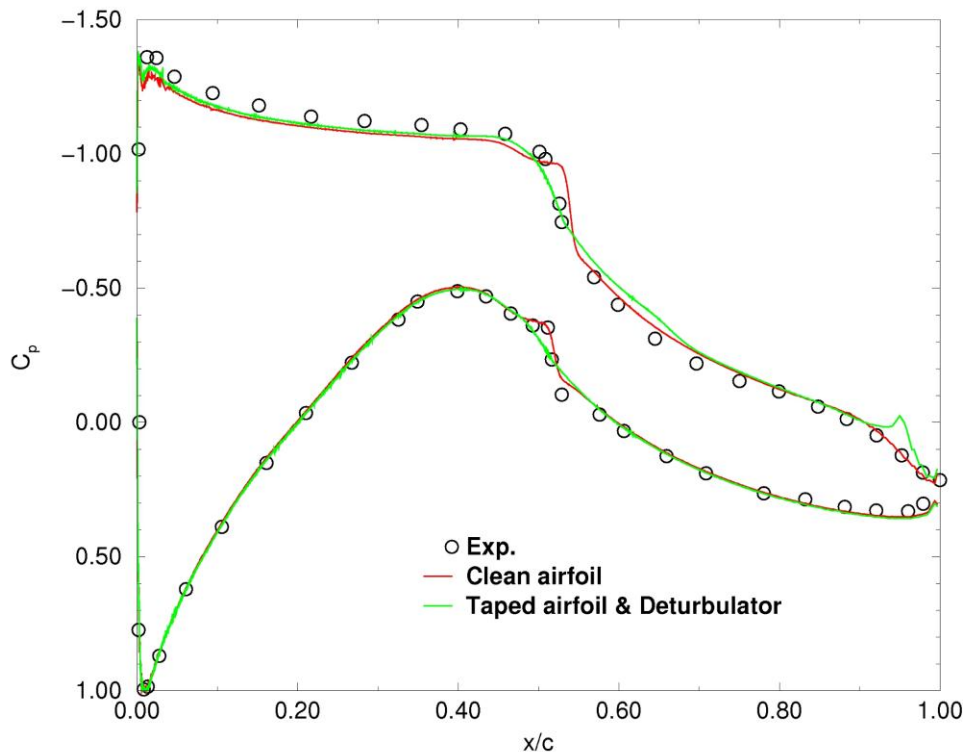
Figure 13. Distribution of Pressure Coefficients

Within the boundary layer of the airfoil upper surface, the simulation predicated the onset of flow separation at x/c=0.50, and the separated flow experienced laminar-to-turbulent transition and reattached at x/c=0.53 to form a laminar separation bubble as shown in Fig. 14. This separation bubble is visualized by the stream-wise velocity vectors and the two vertical lines in Fig. 14 marked the length of the separation bubble. After the separation point, skin friction dropped dramatically attributing (Fig. 15) to the laminar separation bubble. Following the laminar-

American Institute of Aeronautics and Astronautics

turbulent transition of the separated shear layer, flow becomes turbulent characterized with higher turbulent kinetic energy, higher shear and more effective in mixing. The LSL scheme is to tackle this region by attenuating turbulent mixing. Therefore, the kinetic energy of flow is not enough to sustain the random fluctuations against the viscous damping and laminar flow is able to continue to exist. In this case, the LSL method is applied to a range from the flow reattachment point to the trailing edge, within the viscous sub-layer. An upper limiter of turbulent length scale $ls_{limit} = 0.0015$ m is specified.   Comparing the skin friction coefficients in Fig 15, the LSL method is effective in extending the laminar flow beyond the original transition point for a significant distance. As a result, lower shear stress is realized over a wide section downstream of the laminar separation bubble.
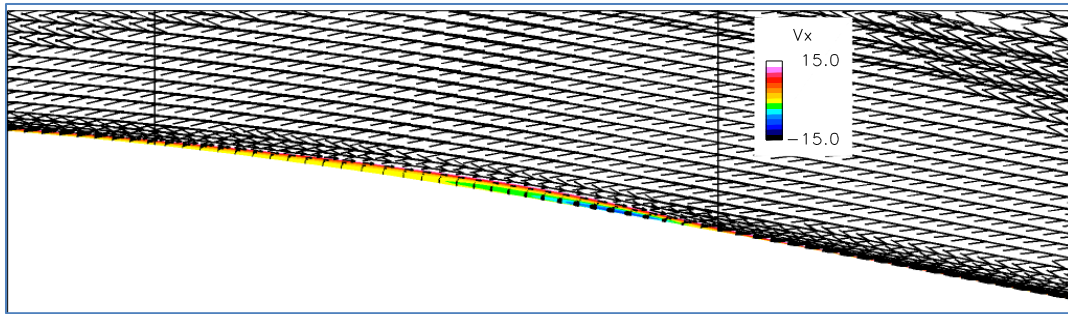
Figure 14. Laminar Separation Bubble on the Upper Surface
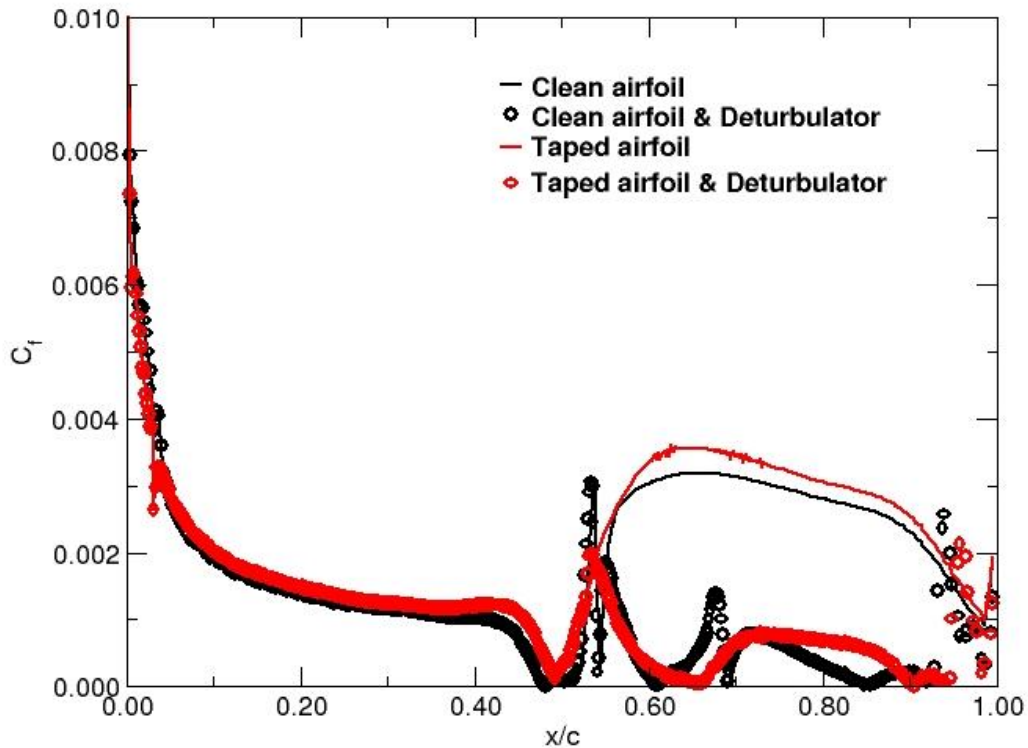
Figure 15. Distribution of Skin Friction Coefficient on the Upper Surface

However, two problems of the aerodynamic performance rise in this LSL simulation. First, the reduction of skin friction drag is overwhelmed by the increase of pressure drag, (summarized in Table 1), which leads to a lower L/D value. Second, the boundary layer treated by the LSL method becomes less stable and turbulent boundary layer separations occurred.

According to the applications of Sinha Deturbulator, it is often necessary to apply a thin tape to the leading edge of a wing (Fig. 8a, Ref. 6). Its purpose is to present a small rear-facing step to precondition the flow as a necessary condition for Deturbulator operation. In an effort to resolve those issues, a backward-facing step of 50 μm in depth is introduced at 3.2% chord from the leading edge on both the upper and lower surface. An unstructured mesh for this modified geometry is generated. A close up view of the backward-facing step is presented in Fig.16.
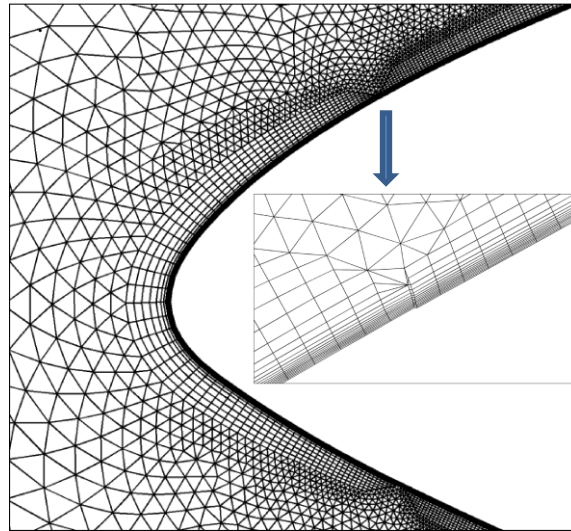
Figure 16. Mesh of S809 with a Backward-Facing Step of 50 μm at 3.2% Chord
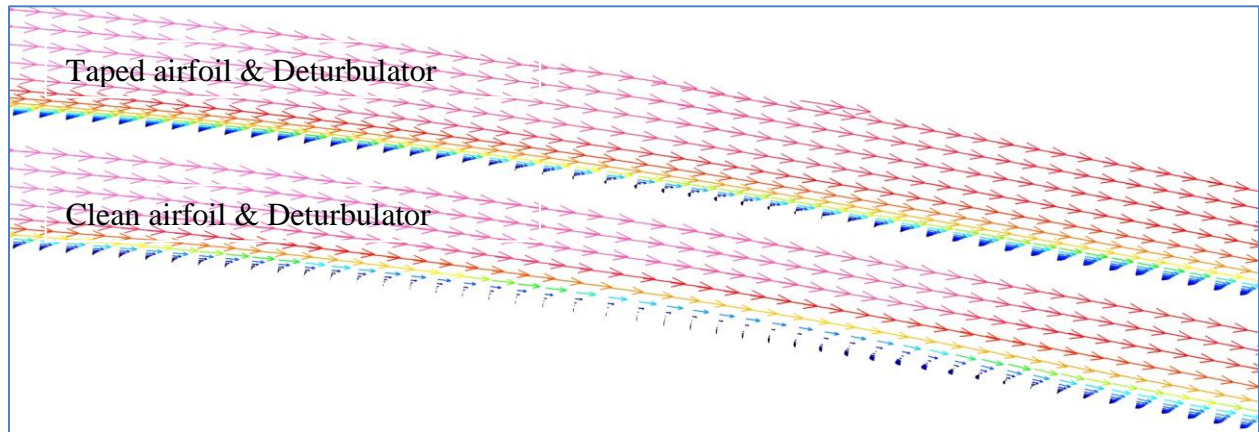
Figure 17. Effect of the Backward-Facing Step on the Laminar Separation Bubble

Two simulations are conducted on this taped airfoil, one uses the TSM turbulence model to obtain a baseline flow, and whereas another one employs the LSL method to mimic the Deturbulator treated airfoil. Figure 17 compares the performance of the Deturbulator on the clean airfoil and the taped airfoil. On the taped airfoil, the laminar separation bubble is shrunk in terms of its length and thickness. In the second case of this taped airfoil, the LSL is applied to the upper surface between the flow reattachment point and the trailing edge. The skin friction coefficients on the upper surface of the taped airfoil are compared with solutions of the clean airfoil geometry in Fig. 15. The predicated skin friction showed that the Deturbulator-treated section experienced lower shear stress all the way to about 95% chord near the trailing edge. Thereafter, shear stress increased due to the trailing edge turbulent boundary layer separation. Figure 17 visualized the streamwise velocity vectors shaded by the its magnitude. It indicated that the backward-facing step at the airfoil leading edge restrained the formation of the laminar separation bubble. This is also reflected by its pressure distribution in Fig. 15, in which the pressure plateau, a typical feature of the laminar separation, has vanished.

To summarize the aerodynamic performance of each case, the integrated lift and drag forces, as well as the skin friction drag are listed in Table 1. The airfoil treated with a tape at the leading edge and with the Deturbulator from flow reattachment point to trailing edge achieved the L/D enhancement. Compared to the clean S809 airfoil, the above treatments reduced the skin friction drag by 20% and increased the lift by 2.57%. This reduction in skin friction drag is able to compensate the slight increase in pressure drag.

Table 1. Integrated Aerodynamic Forces

Case	CFD modeling	Lift C_l	Drag C_d	Skin Friction Drag	L/D
Clean airfoil	TSM	0.7411	0.01369	0.00391	54.14
Clean airfoil + Deturbulator	TSM + LSL	0.7571	0.01408	0.00277(29% reduction)	53.76
Taped airfoil	TSM	0.7428	0.01365	0.00427	54.41
Taped airfoil + Deturbulator	TSM + LSL	0.7607	0.01376	0.00313(20% reduction)	55.28

V. Summary and Conclusions

The effect of large-eddy breakup due to a Flexible Composite Surface Deturbulator device has been modeled in Loci/CHEM, a RANS CFD code, by limiting the turbulence length scale within a zone of influence. Using the aforementioned modifications to the BSL turbulence model wake velocity magnitudes have been computed for an inclined Deturbulator strip. Computed values have been compared to wind-tunnel measurements of the same setup using Deturbulator treated and rigid strips. The most significant result is in the prediction of an extension of the low velocity region of the wake when a Deturbulator is specified (i.e., LSL) instead of a rigid clean strip (i.e., BSL). This supports the hypothesis that the Deturbulator stagnates the separated wake by breaking up large eddies. Even though measured and predicted wake velocity profiles do not quantitatively agree, both display the same qualitative trends resulting from Deturbulator use.

The 30° angle of the Deturbulator wind deflector used in this exploratory study has been subsequently found to be too high. This results in introducing additional vorticity just behind the trailing edge. This vorticity negated the effect of the Deturbulator. Additional measurements and simulations are planned for lower angles where the flow exits smoothly around the trailing edge.

For the airfoil S809 a combination of a backward facing step (i.e., leading edge tape) and TSM-LSL simulated Deturbulator yielded 20% less skin friction over 95% of the chord and low enough trailing edge pressure drag to keep the overall drag lower than the base airfoil. This also increased the lift of the airfoil resulting in increased L/D. The Deturbulator modified the laminar separation bubble and the near-wall velocity profiles to increase the local freestream velocity. This agrees qualitatively with surface oil flow visualizations of Deturbulated flows (e.g., Fig 14 in Ref 10).

Additional boundary layer measurements over the Deturbulator will be needed to refine this modeling by better specifying user-defined parameters.

Acknowledgments

References

[1]Sinha, S.K., "System and Method for Using a Flexible Composite Surface for Pressure-Drop Free Heat Transfer Enhancement and Flow Drag Reduction," U.S. Patent No. 7,422,051, September 9, 2008.

[2]Sinha, S.K., and Ravande, S.V., "Sailplane Performance Improvement Using a Flexible Composite Surface Deturbulator," AIAA Paper 2006-0447, 44th AIAA Aerospace Sciences Meeting, Reno, Nevada, January 9-12, 2006.

[3]Sinha, S.K., and Sinha, S.B., "In Fleet Testing of Fuel Saving Measures," *SAE International Journal of Commercial Vehicles, December 2010* No.3, pp. 323-331.

[4]Tennekes, H. and Lumley, J.L., *A First Course in Turbulence*, The MIT Press, Cambridge, MA. 1989.

[5]Walsh, M.J., Anders, J.B. and Hefner, J.N., "Combined Riblet and LEBU Drag Reduction System," U.S. Patent 4,706,910, November 17, 1987.

[6]Sinha, S.K., and Hyvarinen, "Flexible-Wall Turbulence Control for Drag Reduction on Streamlined and Bluff Bodies," AIAA Paper 2008-4207, 4th Flow Control Conference, Seattle, Washington, 23-26 June 2008.

[7]Sinha, S.K., "Deturbulator Enhanced Wind Deflector," US Provisional Patent Application 61/466344, March 22, 2011.

[8]http://www.sinhadeturb.com

[9]Johnson, R.H., "A Flight Test Evaluation of the Sinha Wing Performance Enhancing Deturbulators ," *SOARING and Motorgliding Magazine*, The Journal of the Soaring Society of America Inc., Vol. 71, No.5, May 2007, pp. 35-41.

[10]Sinha, S.K. and Hendrix, J., "Obtaining Extremely High Lift to Drag Ratios with Flexible-Wall Turbulence Control" AIAA Paper 2009-0896; 47th AIAA Aerospace Sciences Meeting, Orlando, FL, Jan 5-8, 2009.

[11]Sinha, S.K., "Improving Fuel Efficiency of Tractor Trailer Trucks with Deturbulator Aero-Drag Reduction" SAE 2008 Commercial Vehicles Congress, October 7-9, 2008 (SAE Paper 2008-01-2602).

[12]Luke, E., and Cinnella, P., "Numerical Simulations of Mixtures of Fluids Using Upwind Algorithms", *Computers and Fluids*, Vol. 36, pp. 1547-1566, 2007.

[13]Tong, X-L., and Luke, E., "Turbulence Models and Heat Transfer in Nozzle Flows," *AIAA Journal*, Volume 42, Number 11, November 2004, pp. 2391-2393, 2004

[14] Gaither, J.A., Marcum, D.L., and Mitchell, B., "SolidMesh: A Solid Modeling Approach to Unstructured Grid Generation," 7th International Conference on Numerical Grid Generation in Computational Field Simulations, Whistler, BC, 2000.

[15]Marcum, D.L., "Efficient Generation of High Quality Unstructured Surface and Volume Grids," *Engineering with Computers*, 2001. Vol. 17, No. 3, 2001, pp. 211-233.

[16]Marcum, D.L. and Gaither, J.A., "Mixed Element Type Unstructured Grid Generation for Viscous Flow," AIAA paper 99-3252, 14th AIAA Computational Fluid Dynamics Conference, Norfolk, VA.

[17]Menter, F.R., "Two-Equation Eddy-Viscosity Turbulence Models for Engineering Applications," *AIAA Journal*, Vol. 32, No.8, August 1994, pp. 1598-1605.

[18]Walters, D.K. and Cokljat, D., "A Three-Equation Eddy-Viscosity Model for Reynolds-Averaged Navier-Stokes Simulations of Transitional Flow," *Journal of Fluids Engineering*, Vol. 130, No. 12 pp. 121401.1-121401.14, 2008.

[19]Somers, D.M., "Design and Experimental Results for the S809 Airfoil", NREL/SR-440-6918, January 1997.

American Institute of Aeronautics and Astronautics